ELSEVIER

Biophysical Chemistry 107 (2004) 107–116

Biophysical Chemistry

www.elsevier.com/locate/bpc

Scanning tunneling spectroscopy investigation of self-assembled plastocyanin mutants onto gold substrates under controlled environment

L. Andolfi[a,b], G.W. Canters[b], M.Ph. Verbeet[b], S. Cannistraro[a,*]

[a]*Biophysics and Nanoscience Group, INFM, Dipartimento di Scienze Ambientali, Università della Tuscia, Largo dellUniversit, Viterbo I-01100, Italy*

[b]*Leiden Institute of Chemistry, Gorlaeus Laboratoria, Leiden University, The Netherlands*

Received 25 July 2003; received in revised form 26 August 2003; accepted 28 August 2003

Abstract

The study of the electronic conduction through plastocyanin (PC) mutants assembled on a gold surface has been addressed by scanning tunneling spectroscopy. The two mutants exploit a single thiol group (PCSH) or a disulfide bridge (PCSS) to covalently bind at gold surface. The *I–V* measurements were performed by positioning the STM tip on top of a single molecule and sweeping the bias potential between ± 1 V, under both ambient and controlled atmosphere. For PCSS, under ambient conditions, asymmetric *I–V* characteristics were obtained, which disappear under nitrogen atmosphere. PCSH, instead shows a symmetric *I–V* relation in air and under nitrogen environment. Here, as factors underlying this distinct electron conductive behaviour, a potential role for hydration water molecules and for copper redox levels are discussed.

Keywords: Redox proteins; STM; STS; Adsorption on gold; Molecular conduction; Plastocyanin

1. Introduction

The incorporation of redox proteins and enzymes in functional hybrid systems such as bioelectronic devices is one of the most challenging goals in bio-nanotechnology [1–3]. The redox macromolecules display many advantages, i.e. nanometer size, mechanical flexibility, self-assembling ability, suitable tailoring by mutagenesis, substrate recognition and binding capability and more importantly, they can facilitate electron transfer. In this context, the study of heterogeneous electron transfer between metalloproteins and the electrode surface has received increasing attention [4–6]. In recent years progress in this area has been achieved by the use of scanning tunneling microscopy (STM). On the one hand, reproducible images of well resolved single redox proteins self-assembled on gold under various environmental conditions have been obtained [7–14], and on the other hand, insight in the electron transfer properties of a single molecule have been achieved [9,15]. Direct information on biomolecular conduction can be

*Corresponding author. Tel.: +39-0761-357136; fax: +39-0761-357179.

E-mail address: cannistr@unitus.it (S. Cannistraro).

0301-4622/04/$ - see front matter © 2003 Elsevier B.V. All rights reserved.
doi:10.1016/j.bpc.2003.08.012

obtained through scanning tunneling spectroscopy (STS) experiments. Indeed, such an approach widely exploited for studying molecular conduction through small organic molecules [16–21], has been recently extended also to redox active biological macromolecules such as cytochrome *c* [22], copper proteins [9] and photosynthetic complexes [23,24]. In a typical STS experiment, once a molecular image has been obtained and tunneling current and bias voltage have been selected, the tip is accurately repositioned on top of the chosen molecule. The engaging parameters correspond to a tunneling resistance normally of the order of 10^9 Ω and a particular tip-substrate distance. Under these conditions, the bias is swept between positive and negative values and the current is registered after the feedback loop has been disabled. Generally, the *I–V* characteristics appear to be linear for small voltages [25], while a marked asymmetry sometimes is observed at higher voltages (at approx. ±1 V). The origin of the *I–V* asymmetry has been ascribed to various mechanisms: Coulomb blockade [26,27], geometric asymmetry of the molecular junction [28,29], involvement of molecular orbitals [30] including redox levels for redox-active molecules [31–36]. The *I–V* asymmetry is also a fundamental feature related to a rectifying behaviour [37,38], which deserves some interest in the construction of molecular electronic devices.

In a recent work [9], we have performed STM/STS experiments on two poplar plastocyanin mutants. The mutants were designed for immobilization on gold surface specifically involving either a disulfide bridge (PCSS) or a single carboxy-terminal thiol group (PCSH). Both anchoring groups are placed in a protein surface area opposite to the Cu active site [8,9]. Despite similar macromolecular structures and gold binding capabilities, they exhibited different *I–V* characteristics in air, with a marked *I–V* asymmetry for PCSS and a quite symmetric *I–V* relation for PCSH [9]. Due to the robust binding to gold and to the retention of redox activity [39], these two mutants appear very good candidates for implementation in biomolecular devices. For this reason, a better understanding of possible factors influencing their conduction towards the electrode is required. In the present work, we have revisited the STS experiments on PCSS and PCSH in ambient, controlled atmosphere and with some attempts also in water.

Under ambient conditions, the asymmetric *I–V* characteristic was confirmed for the PCSS mutant, while under nitrogen atmosphere the *I–V* asymmetry almost disappeared, indicating that hydration water plays very likely, a role in determining the conductive properties of the protein. Interestingly, for the PCSH mutant a symmetrical *I–V* relation was obtained both in air and under nitrogen atmosphere.

2. Experimental section

Design, expression and purification of both plastocyanin mutants were carried out as described previously [8,9]. STM images were acquired by a Picoscan STM apparatus (Molecular Imaging Co.) equipped with a Picostat (Molecular Imaging Co.) bipotentiostat. A 10-μm scanner with a final preamplifier sensitivity of 1 nA/V was used for STM measurements. Images were acquired both in air and under nitrogen atmosphere in constant current mode, using mechanically cut Pt/Ir tips. Gold substrates deposited on mica (Molecular Imaging) were flame-annealed to obtain recrystallized terraces. STM analysis (not shown here) confirmed the presence of atomically flat Au(111) terraces, a few 100 nm in size. The gold coated substrates were incubated in 64 μM protein solution in 20 mM sodium phosphate buffer at pH 6.0 at 4 °C for various lengths of times. After incubation, the samples were gently rinsed and blown dry with a jet of pure dry nitrogen.

Current–Voltage spectra were obtained starting at a set point of 50 pA and 200 mV bias (tip positive). The bias was swept over ±1 V and a single sweep was collected in 0.01 s. Each single *I–V* spectrum acquired on a single protein consisted of an average over 10 consecutive sweeps. The measurements were repeated for a number of times with different Pt/Ir tips and on different samples. For STS under controlled atmosphere, the sample was sealed into a closed compartment and flushed for 2 h with ultrapure dry nitrogen gas before starting the measurements. During the measure-

ments, the chamber was flushed continuously with pure dry nitrogen. Fluid tunneling spectra were run under pure (18.2 MΩ) water; etched Pt/Ir tips with a leakage <10 pA (Molecular Imaging) were used.

3. Results and discussion

In Fig. 1, representative STM images of PCSS and PCSH mutants on Au(111) in ambient condition are shown. Single molecules on the gold substrate are clearly discernible and can be visualized at different substrate coverage. The lateral dimension of these single molecules well agrees with the crystallographic values of plastocyanin showing a diameter of approximately 4.0 nm [40], and in addition no substantial size differences between the two mutants could be observed. The STM images appear to be stable and reproducible even after repetitive scans. Therefore, a robust binding of the protein molecules to Au(111) substrate is confirmed.

The features of these images closely resemble those already obtained in our previous studies [8,9], where the presence and functionality of plastocyanin mutant molecules bound to gold surface have been further assessed by cyclic voltammetric studies, which provided an electrochemical response consistent with redox-active immobilized plastocyanin molecules [39]. In agreement with our previous work [9], the vertical size of PCSS and PCSH is ranging between 0.5 and 0.7 nm, as measured by the tip retraction along the *z*-axis and shown in the cross section profile of Fig. 1. This height value is significantly smaller than that expected (approx. 2.8 nm) for PC anchored to gold via either the disulfide bridge (PCSS) or via the single thiol (PCSH). Indeed, the vertical topological height for both mutants immobilised on gold surface can be recovered by tapping mode AFM [9].

The considerable reduction of the physical height of biomolecules is a common feature encountered in STM images of organic material. The reason for the discrepancy between the physical and the apparent height observed in the STM images is still an open question and is somewhat connected to the mechanism of image contrast

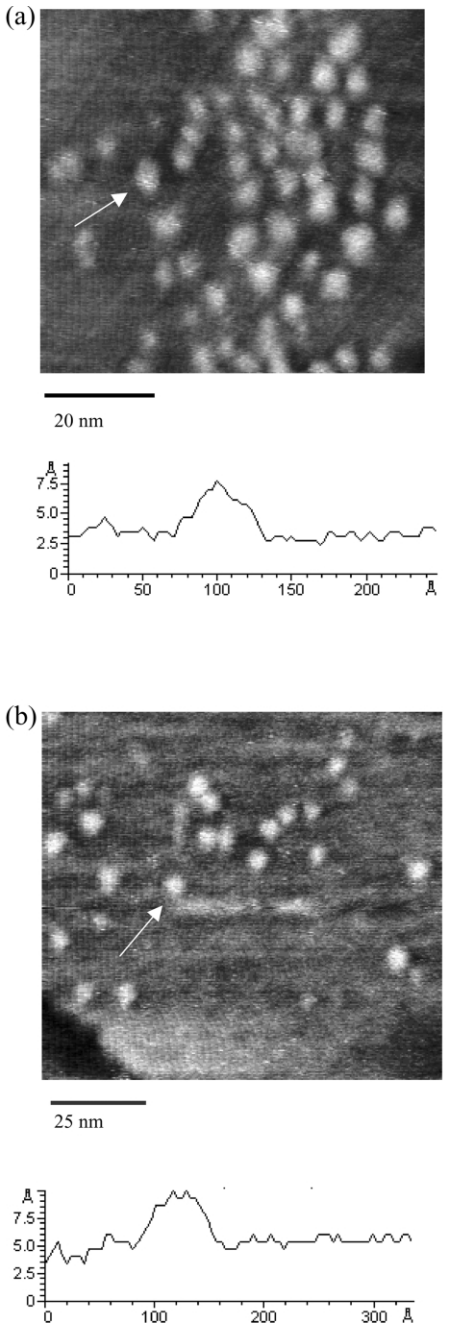

Fig. 1. Constant current STM image of PCSS (a) and PCSH (b) on gold surface in ambient condition scan area: 68×68 nm^2 and 100×100 nm^2. Tunneling current 50 pA, bias voltage 200 mV (tip positive), scan rate 5 Hz. Molecule cross section profiles are shown in the lower panels.

formation. This is especially relevant when imaging soft biological material. The apparent height of a biomolecule observed in the STM image is related to the tip retraction along the z-axis, which is, in turn, connected with the biomolecular conduction and with the starting tip-sample distance. Recently, we have faced this aspect and found that in our engaging conditions, i.e. 50 pA of tunneling current and 200 mV bias tunneling starting distances of approximately 3 and 6 nm in water and ambient condition, respectively, could be estimated [41]. According to these results, we can reasonably assume that the tip does not touch the protein during the imaging, thereby allowing to acquire $I-V$ characteristics of plastocyanin single molecules in a non-invasive way.

The STS measurements were performed by positioning the tip on top of the redox protein, the feedback loop was temporarily disengaged and the tunneling current was monitored as the sample bias was ramped in the range of ± 1 V. The current direction through the molecule will then vary according to the bias polarity, i.e. from the substrate to the tip for negative values and from tip to substrate for positive ones. Each single $I-V$ spectrum acquired on a single protein consists of the average over 10 consecutive bias sweeps. The measurements were repeated for a large number of molecules. The bias sweeps, obtained from ambient STS experiments, were averaged and the resulting curves for PCSS (700 bias sweeps), PCSH (720 bias sweeps) and Au(111) (800 bias sweeps) with their error bars (S.D. of the mean) are plotted in Fig. 2.

First, a slight asymmetry in the $I-V$ relation of gold (Fig. 2c) appears in the range of ± 1 V. This can be attributed to the contribution of the sharp tip apex to the $I-V$ spectra and has been treated theoretically [42]. Similarly, a slight asymmetric $I-V$ relation for PCSH is observed (Fig. 2b). However, this feature is almost indistinguishable from that of gold within the experimental error. At variance, PCSS shows a significant asymmetry (Fig. 2a) when compared to gold with a confidence level of 99.7%.

As mentioned before, many mechanisms can be invoked to explain $I-V$ asymmetry. In the case of redox active molecules a particular attention has been paid to the involvement of redox electronic levels [19,20,22]. Actually, the derivative of current–voltage data has been put into relationship with the molecular density of the states (DOS), which is believed to be responsible for mediating the enhanced tunneling [43]. In this context, several studies have suggested that the pronounced asymmetry in the $I-V$ characteristics is due to an interplay between the position of the molecular redox levels and the tip-substrate Fermi level in connection to the bias polarity [19–22]; such an hypothesis being still amply debated.

However, in the case of biomolecules it should be taken into account the water layer which is always present at the sample surface. This may play a considerable role in the tunneling mechanism [44–46]. In particular, the presence of hydration water has been suggested to affect image contrast formation especially for insulating samples such as biomolecules [47,48]. Indeed, it appears conceivable that the polarization of the water molecules in the high electric field of the tunneling junction may have a different effect on conduction when the current runs from substrate to the tip or vice versa depending on the polarity of the bias; the orientation of the water molecules inside the STM junction having been proposed to influence the electron tunneling [49]. In fact, at positive sample bias and under high electric field the first water layer at the sample surface is probably polarized with the oxygen groups facing the electrode. This ordering creates a lateral compression of the layer, which prohibits through space tunneling. In the case of a negative sample bias, the water molecule are polarised to a lesser degree, allowing an easier tunneling with a lower tunneling barrier.

For this reason a particular attention should be paid to the role of the water layer at the sample interface when studying the conduction of biomolecule. Therefore, we acquired tunneling spectra under nitrogen atmosphere, where we may reasonably assume that the water layer at the sample interface normally present under ambient conditions is strongly reduced. STM images under nitrogen atmosphere were acquired for PCSS and PCSH as shown in Fig. 3. The images show individual molecules spread on the metallic sur-

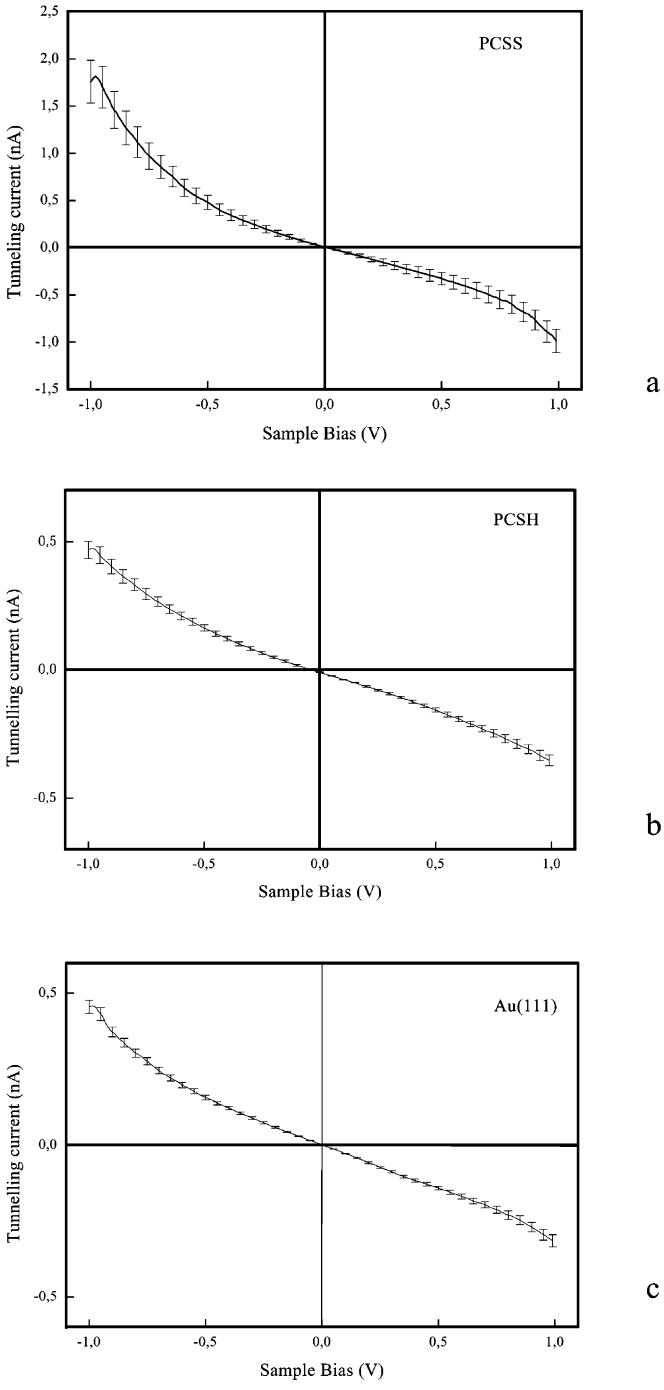

Fig. 2. *I–V* curves recorded in ambient conditions on PCSS molecules (a) on PCSH (b) and Au(111) (c). The engage tunneling current and bias voltage are 50 pA and 200 mV (tip positive). The error bars represent the standard deviation of the mean, which has been calculated at each V point, but for clarity the error bar is shown every four points.

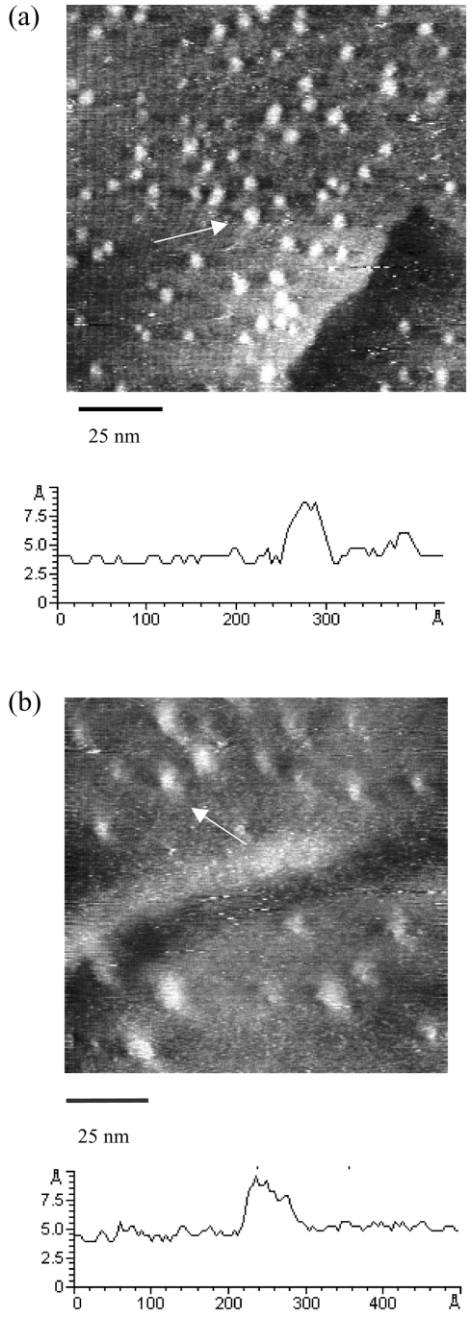

Fig. 3. Constant current STM images of PCSS (a) and PCSH (b) on Au(111) under nitrogen atmosphere scan area: 125×125 nm^2 and 115×115 nm^2. Tunneling current 50 pA, bias voltage 200 mV (tip positive), scan rate 5 Hz. Molecule cross section profiles are shown in the lower panels.

face, with lateral dimensions of approximately 4.0 nm close to what is expected from the X-ray crystallography data [40]. The estimated vertical size of PCSS and PCSH appears again to be in the range of 0.5–0.7 nm, similar to what is observed under ambient imaging and significantly smaller than the crystallographic value. The imaging in a controlled environment appears stable and reproducible allowing thus to collect single molecule tunneling spectroscopic data. The $I-V$ curves under nitrogen were taken according to the previous experimental procedure. All the bias sweeps were averaged and the resulting curves for PCSS (390 bias sweeps), PCSH (290 bias sweeps) and Au(111) (500 bias sweeps) with their error bars are plotted in Fig. 4.

The $I-V$ relation obtained for gold under nitrogen is quite symmetric. In the case of PCSH, the $I-V$ curve closely resembles that obtained under ambient conditions, while the asymmetry observed for PCSS molecules has almost disappeared with a concomitant decrease of the recorded current. The slight differences between the $I-V$ data obtained for both mutants and that obtained on gold under nitrogen atmosphere do not appear to be significant when considering a confidence level of 99.7%.

In the light of the previous observations, it would be of interest to probe the conductive behaviour of these proteins under fluid condition, which represents the most suitable environment for studying the functionality of biomolecules. However, in aqueous media the variation of the bias might lead to some electrochemical interferences at the metal (Pt/Ir) tip. This may impose a limit to the tip-substrate potential that can be applied due to the occurrence of leakage problems. This may also compromise the reproducibility of the STS measurements. We present some attempts that we made in pure water. An example of the obtained $I-V$ relation acquired under pure water on Au(111) surface over a ±1 V range is shown in Fig. 5. Curve (a) is an average over 250 sweeps performed on a gold surface while curve (b) is an average over 20 sweeps with the same tip. It is clearly visible that the $I-V$ curves on gold already can change in time possibly because of leakage

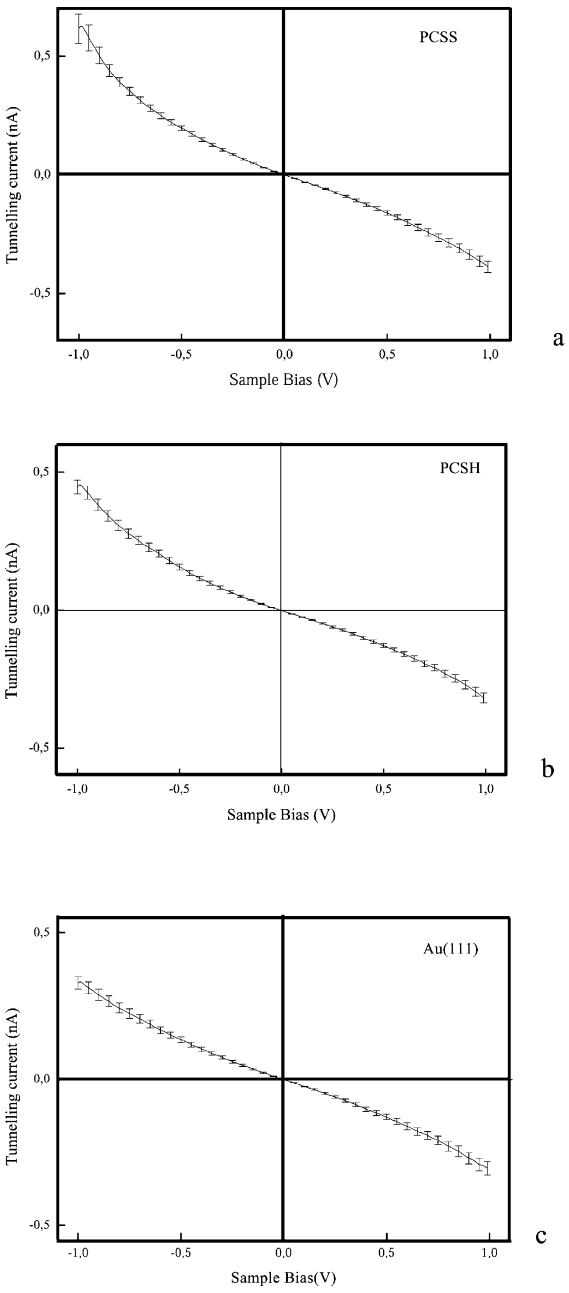

Fig. 4. *I–V* curves recorded under nitrogen atmosphere on PCSS molecules (a) on PCSH (b) and Au(111) (c). The engage tunneling current and bias voltage are 50 pA and 200 mV (tip positive). The error bars represent the standard deviation of the mean, which has been calculated at each V point, but for clarity the error bar is shown every four points.

problems. Therefore, a more accurate investigation, probably under electrochemical control is needed.

Comparing the results obtained in the two environments, some observations stand out. For PCSS, the asymmetry in the *I–V* characteristics observed in the STS experiments under ambient conditions is no more present, when the experiments are carried out under nitrogen atmosphere at low ambient humidity. Furthermore, and strikingly enough, *I–V* curve related to PCSH is symmetric under both conditions. Since we may be confident that under nitrogen atmosphere the water layer at the sample interface is substantially reduced [50], the obtained results seem to point out that the water content of the sample may affect the registered *I–V* characteristics for the adsorbed plastocyanin mutants. Nevertheless, this appears puzzling if we admit that the hydration water layer present under ambient conditions could be responsible for the asymmetry in the case of PCSS; being not clear why in the same environment, PCSH does not display this asymmetry. It is hard to conceive that PCSH would retain a different level of humidity with respect to the similar mutant PCSS. We might invoke some difference between the orientation and interfacing of the two mutant proteins towards the electrode surface. In the case of PCSH, binding to gold through the thiol group at the carboxy-terminal free end might lead to a less hindered protein surface–electrode coupling than that obtained via the S–S bridge. In addition, we might speculate about the possibility that the electronic levels of the copper ion could be involved in generating the asymmetry [19,20,22]; but in that case a different oxidation state should be admitted for the two mutants.

4. Conclusion

Imaging and spectroscopic data of two plastocyanin mutants self-assembled on gold surface via a single thiol group or a disulfide bridge were acquired at level of single molecule by using high resolution STM. Under ambient conditions, the two mutants give rise to different *I–V* behaviour. Particularly, an asymmetric *I–V* curve for PCSS and a symmetric *I–V* curve for PCSH were obtained. Under nitrogen, the asymmetric *I–V*

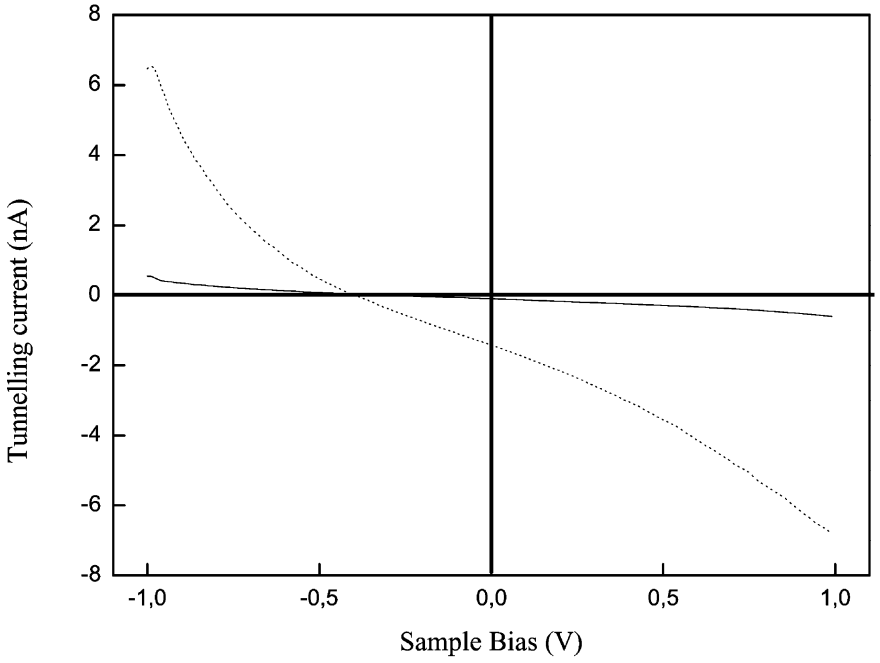

Fig. 5. Repetitive *I–V* curve recorded in water milliQ on Au(111) by using a Pt/Ir tip with a leakage <10 pA. The straight line is obtained by averaging the first 250 *I–V* sweeps. The dotted line resulted by averaging 20 consecutive *I–V* sweeps after acquiring the first 250 sweeps. Engaging tunneling current and bias voltage are 50 pA and 200 mV (tip positive).

characteristics observed for the PCSS mutant disappear, while the PCSH preserves essentially a symmetric *I–V* relation.

At present we are unable to distinguish among the possible mechanisms, but these results point out that particular care should be exercised when performing conductive studies on biological macromolecules by the STS approach, in particular, concerning tip-sample distance and hydration state.

Acknowledgments

This work has been partially supported by the 'Molecular Monodevices' FIRB-MIUR Project and by the EC Project SAMBA (V Frame FET).

References

[1] C. Joachim, J.K. Gimzewski, A. Aviram, Electronics using hybrid-molecular and mono-molecular devices, Nature 408 (2000) 541–548.

[2] I. Willner, B. Willner, Biomaterials integrated with electronic elements: en route to bioelectronics, Trends Biotechnol. 19 (2001) 222–230.

[3] G. Gilardi, A. Fantuzzi, Manipulating redox systems: application to nanotechnology, Trends Biotechnol. 19 (2001) 468–476.

[4] L.J.C. Jeuken, A.K. Jones, S.K. Chapman, G. Cecchini, F.A. Armstrong, Electron-transfer mechanisms through biological redox chains in multicenter enzymes, J. Am. Chem. Soc. 124 (2002) 5702–5713.

[5] G. Gilardi, A. Fantuzzi, S.J. Sadeghi, Engineering and design in the bioelectrochemistry of metalloproteins, Curr. Opin. Struc. Biol. 11 (2001) 491–499, References therein.

[6] Q.C. Li, P.A. Mabrouk, Spectroscopic and electrochemical studies of horse myoglobin in dimethyl sulfoxide, J. Biol. Inorg. Chem. 8 (2003) 83–94.

[7] Q. Chi, J. Zhang, J.U. Nielsen, E.P. Friis, I. Chorkendorff, G.W. Canters, et al., Molecular monolayers and interfacial electron transfer of *Pseudomonas Aeruginosa* Azurin on Au (111), J. Am. Chem. Soc. 122 (2000) 4047–4055.

[8] L. Andolfi, S. Cannistraro, G.W. Canters, P. Facci, A.G. Ficca, I.M.C. van Amsterdam, et al., A poplar plastocyanin mutant suitable for adsorption onto gold surface via disulfide bridge, Arch. Biochem. Biophys. 399 (2002) 81–88.

[9] L. Andolfi, B. Bonanni, M.Ph. Verbeet, G.W. Canters, S. Cannistraro, Scanning probe microscopy charcteriza-

tion of gold-chemisorbed poplar plastocyanin mutants, Surf. Sci. 530 (2003) 181–194.
[10] P. Facci, D. Alliata, S. Cannistraro, Potential-induced resonant tunneling through a redox metalloprotein probed by electrochemical scanning probe microscopy, Ultramicroscopy 89 (2001) 291–298.
[11] J.J. Davis, H.A.O. Hill, The scanning probe microscopy of Metalloproteins and metalloenzymes, Chem. Commun. (2002) 393–401.
[12] D. Djuricic, H.A.O. Hill, K.K.-W. Lo, L.-L. Wong, A scanning tunneling microscopy (STM) Investigation of complex formation between Cytochrome $P450_{cam}$ and Putidaredoxin, J. Inorg. Biochem. 88 (2002) 362–367.
[13] J. Zhang, Q. Chi, S. Dong, E. Wang, In situ electrochemical scanning tunneling microscopy investigation of structure for horseradish peroxidase and its electrocatalytic property, Bioelectrochem. Bioenerg. 39 (1996) 267–274.
[14] O. Cavalleri, C. Natale, M.E. Stroppolo, A. Relini, E. Cosulich, S. Thea, et al., Azurin immobilisation on thiol covered Au(111), Phys. Chem. Chem. Phys. 2 (2000) 4630–4635.
[15] J. Zhang, Q. Chi, A.M. Kuznestov, A.G. Hansen, H. Wackerbarth, H.E.M. Christensen, et al., Electronic properties of functional biomolecules at metal/aqueous solution interfaces, J. Phys. Chem. 106 (2002) 1131–1152.
[16] U. Durig, O. Zuger, B. Michel, L. Haussling, H. Ringsdorf, Electronic and mechanical characterization of self-assembled alkanethiol monolayers by scanning tunneling microscopy combined with interaction-force-gradient sensing, Phys. Rev. Lett. 48 (1993) 1711–1717.
[17] A.S. Blum, J.C. Yang, R. Shashidhar, B. Ratna, Comparing the conductivity of molecular wires with the scanning tunneling microscope, Appl. Phys. Lett. 82 (2003) 3322–3324.
[18] W. Tian, S. Datta, S. Hong, R. Reifenberger, J.I. Henderson, C.P. Kubiak, Conductance spectra of molecular wires, J. Chem. Phys. 109 (1998) 2874–2882.
[19] U. Mazur, K.W. Hipps, Orbital mediated tunneling, inelastic electron tunneling and electrochemical potentials for metal phthalocyanine thin films, J. Phys. Chem. B 103 (1999) 9721–9727.
[20] W. Han, E.N. Durantini, T.A. Moore, A.L. Moore, D. Gust, P. Rez, et al., STM contrast, electron-transfer chemistry and conduction in molecules, J. Phys. Chem. B 101 (1997) 10 719–10 725.
[21] N. Katsonis, A. Marchenko, D. Fichou, Dynamics and spectroscopy of individual C60 molecules adsorbed at the *n*-tetradecane/Au(111) interface, J. Photochem. Photobiol. A Chem. 158 (2003) 101–104.
[22] G.B. Khomutov, L.V. Belovolova, S.P. Gubin, V.V. Khanin, A. Yu Obydenov, A.N. Sergeev-Cherenkov, et al., STM study of morphology and electron transfer features in cytochrome *c* and nanoclusters molecule monolayers, Bioelectrochemistry 55 (2002) 177–181.
[23] P.B. Lukins, T. Oates, Single-molecule high-resolution structure and electron conduction of photosystem II from scanning tunneling microscopy and spectroscopy, Biochim. Biophys. Acta 1409 (1998) 1–11.
[24] P.B. Lukins, Single-molecule electron tunneling spectroscopy of the higher plant light-harvesting complex LHC II, Biochem. Biophys. Res. Commun. 256 (1999) 288–292.
[25] C. Joachim, J.K. Gimzewski, Analysis of low-voltage $I(V)$ characteristics of a single C_{60} molecule, Europhys. Lett. 30 (1995) 409–414.
[26] R.P. Andres, T. Bein, M. Dorogi, S. Feng, J.I. Henderson, C.P. Kubiak, et al., Coulomb staircase at room temperature in a self-assembled molecular nanostructure, Science 272 (1996) 1323–1325.
[27] J. Park, A.N. Pasupathy, J.I. Goldsmith, C. Chang, Y. Yaish, J.R. Petta, et al., Coulomb blockade and the Kondo effect in single atom transistors, Nature 417 (2002) 722–725.
[28] J. Reichert, R. Ochs, D. Beckman, H.B. Weber, M. Mayor, H.V. Löhneysen, Driving current through single organic molecules, Phys. Rev. Lett. 88 (2002) 176804-1–176804-4.
[29] A.W. Ghosh, F. Zahid, P.S. Damle, S. Datta, Insights into molecular conduction from I–V asymmetry, Condens. Matter (2002) 1–4.
[30] S.N. Yaliraki, M. Kemp, M.A. Ratner, Conductance of molecular wires: influence of molecule-electrode binding, J. Am. Chem. Soc. 121 (1999) 3428–3434.
[31] W. Schmickler, Investigation of electrochemical electron transfer reactions with scanning tunneling microscope: a theoretical study, Surf. Sci. 295 (1993) 43–56.
[32] A.M. Kuznetsov, J. Ulstrup, Mechanism of in situ scanning tunneling microscopy of organized redox molecular assemblies, J. Phys. Chem. A 104 (2000) 11 531–11 540.
[33] L. Ottaviano, S. Santucci, S. Di Nardo, L. Lozzi, M. Passacantando, P. Picozzi, Rectifying behavior of silicon phthalocyanine junctions investigated with scanning tunneling microscopy/spectroscopy, J. Vac. Sci. Technol. A 15 (1997) 1014–1019.
[34] S. Zhou, Y. Liu, Y. Xu, D. Zhu, X. Qiu, C. Wang, et al., Rectifying behaviours of Langmuir–Blodgett films of an asymmetrically substituted phthalocyanine, Chem. Phys. Lett. 297 (1998) 77–82.
[35] L.A. Bumm, J.J. Arnold, T.D. Dunbar, D.L. Allara, P.S. Weiss, Electron transport through organic molecules, J. Phys. Chem. 83 (1999) 8122–8127.
[36] A.S. Blum, J.C. Yang, R. Shashidhar, B. Ratna, Comparing the conductivity of molecular wires with the scanning tunneling microscope, Appl. Phys. Lett. 82 (2003) 3322–3324.
[37] C. Krzeminski, C. Delerue, G. Allan, D. Vuillaume, R.M. Metzger, Theory of rectification in a molecular monolayer, Phys. Rev. B 64 (2001) 1–6.
[38] M.L. Chabinyc, X. Chen, R.E. Holmlin, H. Jacobs, H. Skulason, C.D. Friesbie, et al., Molecular rectification

in a metal-insulator-metal junction based on self-assembled monolayer, J. Am. Chem. Soc. 124 (2002) 11 730–11 736.

[39] L. Andolfi, J.J. Davis, M. Ph. Verbeet, G.W. Canters, S. Cannistraro, H.O.A. Hill, The electrochemical characteristics of blue copper protein monolayers on gold, J. Electroanal. Chem. (2003) in press.

[40] M. Milani, L. Andolfi, S. Cannistraro, M.Ph. .Verbeet, M. Bolognesi, The 1.6 Å resolution crystal structure of a mutant plastocyanin bearing a 21–25 engineered disulfide bridge, Acta Cryst. D57 (2001) 1735.

[41] D. Alliata, L. Andolfi, S. Cannistraro, Ultramicroscopy (2003) submitted.

[42] A.I. Onipko, K.F. Bergger, Y.O. Klymenko, L.I. Malysheva, J.J.W.M. Rosink, L.J. Geerligs, et al., Scanning tunneling spectroscopy on π-conjugated phenyl-based oligomers. A simple physical model, Phys. Rev. B 61 (2000) 11 118–11 124.

[43] W. Schmickler, C. Wridig, The investigation of redox reactions with scanning tunneling microscope. Experimental and theoretical aspects, J. Electroanal. Chem. 336 (1992) 213–221.

[44] J.R. Hahn, Y.A. Hong, H. Kang, Electron tunneling across interfacial water layer inside STM junction. Tunneling distance, barrier height and water polarization effect, Appl. Phys. A 66 (1998) S467–S472.

[45] M. Heim, R. Eschrich, A. Hillebrand, H.F. Knapp, R. Guckenberger, G. Cevc, STM based on the conductivity of surface adsorbed water. Charge transfer between tip and sample via electrochemistry in a water meniscus or via tunneling?, J. Vac. Sci. Technol. B 14 (1996) 1498–1502.

[46] M.-B. Song, J.-M. Jang, S.-E. Bae, C.-W. Lee, Charge transfer through thin layers of water investigated by STM, AFM and QCM, Langmuir 18 (2002) 2780–2784.

[47] N. Patel, M.C. Davies, M. Lomas, C.J. Roberts, S.J.B. Tendler, P.M. Williams, STM of insulators with the probe in contact with an aqueous layer, J. Phys. Chem. 101 (1997) 5138–5142.

[48] R. Guckenberger, M. Heim, G. Cevc, H. Knapp, W. Wiegräbe, A. Hillebrand, STM of insulators and biological specimens, based on lateral conductivity of ultrathin water films, Science 266 (1994) 1538–1541.

[49] Y.A. Hong, J.R. Hahn, H. Kang, Electron transfer through interfacial water layer studied by scanning tunneling microscopy, J. Chem. Phys. 108 (1998) 4367–4370.

[50] R.B. Gregory, Protein–solvent Interactions, Marcel Dekker Inc, New York, 1995.